

Microglia in the adult brain arise from Ly-6C^{hi}CCR2⁺ monocytes only under defined host conditions

Alexander Mildner¹, Hauke Schmidt¹, Mirko Nitsche², Doron Merkler¹, Uwe-Karsten Hanisch¹, Matthias Mack³, Mathias Heikenwalder⁴, Wolfgang Brück^{1,5}, Josef Priller^{6,7} & Marco Prinz^{1,7}

Microglia are crucially important myeloid cells in the CNS and constitute the first immunological barrier against pathogens and environmental insults. The factors controlling microglia recruitment from the blood remain elusive and the direct circulating microglia precursor has not yet been identified *in vivo*. Using a panel of bone marrow chimeric and adoptive transfer experiments, we found that circulating Ly-6C^{hi}CCR2⁺ monocytes were preferentially recruited to the lesioned brain and differentiated into microglia. Notably, microglia engraftment in CNS pathologies, which are not associated with overt blood-brain barrier disruption, required previous conditioning of brain (for example, by direct tissue irradiation). Our results identify Ly-6C^{hi}CCR2⁺ monocytes as direct precursors of microglia in the adult brain and establish the importance of local factors in the adult CNS for microglia engraftment.

Microglia are an integral part of the resident mononuclear phagocyte population in the CNS. These cells share many phenotypical and functional characteristics with other tissue macrophages and with peripheral blood monocytes, suggesting that microglia participate in many immune reactions of the brain¹. Microglia continuously monitor their local microenvironment with highly motile processes and constitute the first line of defense against invading pathogens^{2,3}.

Microgliosis is a rather poorly understood process, despite it having a probable role in the pathogenesis of various CNS diseases⁴. One major issue is to determine the extent to which circulating monocytes contribute to the microglial response in the brain. Despite tremendous efforts in the past years, monocyte-derived and resident CNS parenchymal microglia remain virtually indistinguishable on the basis of known immunophenotypic markers, although they might be functionally heterogeneous⁵. Using chimeric mice, in which bone-marrow cells (BMCs) were marked with the green fluorescent protein (GFP), MHC class II, Y chromosome, congenic CD45.1/CD45.2 molecules and others, bone marrow-derived cells were shown to enter the brain during postnatal development and to differentiate into microglia^{6–8}, but not into other glial cell types⁹. Subsequent studies in mice have even demonstrated enhanced microglia engraftment in several disease models, such as spongiform encephalopathies^{10,11}, bacterial meningitis¹², experimental autoimmune encephalomyelitis¹³, Parkinson's disease¹⁴ and Alzheimer's disease^{5,15,16}. Notably, bone marrow-derived microglia appeared to be functionally relevant in the brain; for example, they phagocytosed β -amyloid in Alzheimer's disease transgenic mice, whereas resident microglia seemed to be rather ineffective in removing β -amyloid⁵. All of these chimeric mice studies used total

body irradiation as the conditioning regimen for the bone-marrow transplantation, thereby exposing the brain to potential irradiation-induced changes in the local microenvironment. Indeed, the few studies using nonirradiated parabiotic mice detected substantially less engrafted microglia in the brains¹⁷. Therefore, we designed a set of experiments using bone-marrow chimeric approaches to define the local conditions in the brain that allow the entry of blood-derived monocytes into the CNS and their differentiation into parenchymal microglia.

Furthermore, the direct circulating precursor of microglia in the peripheral blood has not yet been identified *in vivo*. Prevailing concepts view monocytes as intermediary cells that continuously develop in the bone marrow, circulate in the blood and migrate into tissues, where they become local macrophages, dendritic cells or other tissue descendants¹⁸. The identification of monocyte heterogeneity has led to the hypothesis that monocytes commit for specific functions while still in the circulation¹⁹. Indeed, both human and mouse monocytes fall into at least two phenotypically distinct subsets: Ly-6C^{hi} (which are Gr-1⁺CCR2⁺CX₃CR1^{lo}) and Ly-6C^{lo} (which are Gr-1⁻CCR2⁻CX₃CR1^{hi}) mouse monocytes, which correspond to human CD14^{hi}CD16⁻ and CD14⁺CD16⁺ monocytes, respectively^{20,21}. It is generally thought that Ly-6C^{hi} cells preferentially populate sites of experimentally induced inflammation, whereas their Ly-6C^{lo} counterparts can enter lymphoid and nonlymphoid tissues under homeostatic conditions²².

Here we demonstrate that circulating Ly-6C^{hi}CCR2⁺ monocytes are direct circulating precursors of microglia in the blood. Genetic or antibody-mediated depletion of this specific monocyte subtype vastly prevented the recruitment of monocytes into the lesioned brain.

¹Institute of Neuropathology and ²Department of Radiation Oncology, Georg August University, Göttingen, Germany. ³Department of Internal Medicine, University of Regensburg, Regensburg, Germany. ⁴Institute of Neuropathology, Universitätsspital, Zurich, Switzerland. ⁵Institute for Multiple Sclerosis Research, Georg August University, Göttingen, Germany. ⁶Laboratory of Molecular Psychiatry, Charité-Universitätsmedizin Berlin, Germany. ⁷These authors contributed equally to this work. Correspondence should be addressed to M.P. (mprinz@med.uni-goettingen.de).

Received 17 May; accepted 25 October; published online 18 November 2007; doi:10.1038/nn2015

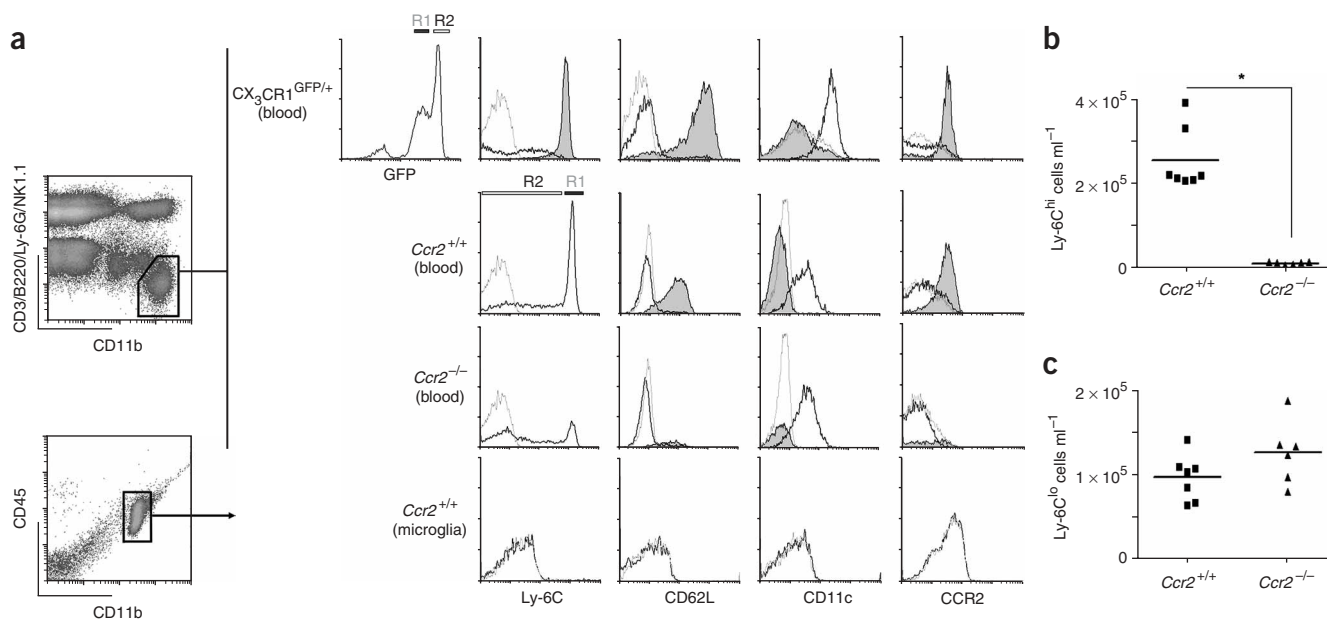


Figure 1 Brain-specific macrophages (microglia) have an immunomarker profile similar to that of resident blood monocytes. (a) Blood monocytes (upper left density plot) of *Ccr2*^{+/+}, *Ccr2*^{-/-} and CX₃CR1^{GFP/+} mice, and *ex vivo*-isolated microglia (lower left density plot) of *Ccr2*^{+/+} mice were characterized by surface expression of the markers Ly-6C, CCR2, CD62L, CD11b and CD11c. Living blood cells were gated to determine the presence of CD11b^{hi}CD3^{lo}B220^{lo}Ly-6C^{lo}NK1.1^{lo} monocytes (upper left). CX₃CR1^{GFP/+} mice were used to distinguish between CX₃CR1^{hi} (R2, Ly-6C^{lo}) and CX₃CR1^{lo} (R1, Ly-6C^{hi}) blood monocytes. Percoll gradient-isolated microglia were gated as a CD45^{lo}CD11b⁺ cell population in the brain (lower left). R2 gates (thick lines) and R1 gates (filled curves) in the blood indicate Ly-6C^{lo} and Ly-6C^{hi} monocytes, respectively. Isotype controls are shown as thin lines. (b) Adult CCR2-deficient mice showed a distinct lack of Ly-6C^{hi} monocytes in the peripheral blood. Each symbol represents one individual mouse. The mean is indicated. Asterisk indicates statistical significance ($P < 0.05$). (c) No significant difference in the amount of Ly-6C^{lo} monocytes was found in the peripheral blood of WT versus *Ccr2*^{-/-} mice. Each symbol represents one individual mouse. The mean is indicated.

Demyelinating and neurodegenerative CNS disease models without blood-brain barrier disruption were not sufficient to induce substantial microglia engraftment during adulthood, but additional host endogenous factors, such as irradiation-induced gene expression, were required to condition the adult brain for microglia engraftment.

RESULTS

Microglia display surface markers of specific monocytes

To test the hypothesis that a distinct subset of circulating monocytes represents the direct precursor of microglia in the adult brain, surface immunomarker expression of microglia was compared with circulating monocyte populations (Fig. 1). Monocytes in the peripheral blood were defined as CD11b^{hi}CD3^{lo}B220^{lo}Ly-6C^{lo}NK1.1^{lo} mononuclear cells by flow cytometry as described previously (Fig. 1a)²³. We took advantage of the CX₃CR1^{GFP/+} mice (GFP is inserted into one allele of the CX₃CR1 locus), which allow division of the Ly-6C^{hi} and Ly-6C^{lo} fractions on the basis of GFP expression levels. Microglia were subsequently defined as being CD45^{lo} and CD11b⁺ according to the literature²⁴. Notably, isolated microglia were CD62L⁻CCR2⁻Ly-6C^{lo}, which was similar to the immunoprofile found on resident Ly-6C^{lo} monocytes. This monocyte population, however, was reported to be CD11c⁺ (ref. 23), which was not the case in isolated adult microglia.

A previous report claimed that the chemokine receptor CCR2 might also be required for the emigration of Ly-6C^{hi}CCR2⁺ monocytes from the bone marrow into the circulation²⁵. Theoretically, this could cause a deficiency of this specific monocyte subpopulation in the peripheral blood stream. To test this hypothesis, we counted the number of Ly-6C^{hi} monocytes in the blood of 8-week-old adult *Ccr2*^{-/-} mice and in age- and sex-matched *Ccr2*^{+/+} mice (Fig. 1b). The amount of Ly-6C^{hi} monocytes was substantially reduced in CCR2-deficient mice

compared with the wild-type (WT) situation (mean \pm s.e.m., $1.2 \pm 0.1 \times 10^4$ cells ml⁻¹ in *Ccr2*^{-/-} and $25.6 \pm 2.8 \times 10^4$ cells ml⁻¹ in WT mice). To ensure that only this specific monocyte subtype was affected, we examined the amount of Ly-6C^{lo} monocytes (Fig. 1c). Notably, we found an unchanged amount of Ly-6C^{lo} monocytes in CCR2-deficient mice compared to WT (mean \pm s.e.m., $12.6 \pm 1.7 \times 10^4$ cells ml⁻¹ in *Ccr2*^{-/-} and $9.7 \pm 1.0 \times 10^4$ cells ml⁻¹ in WT mice).

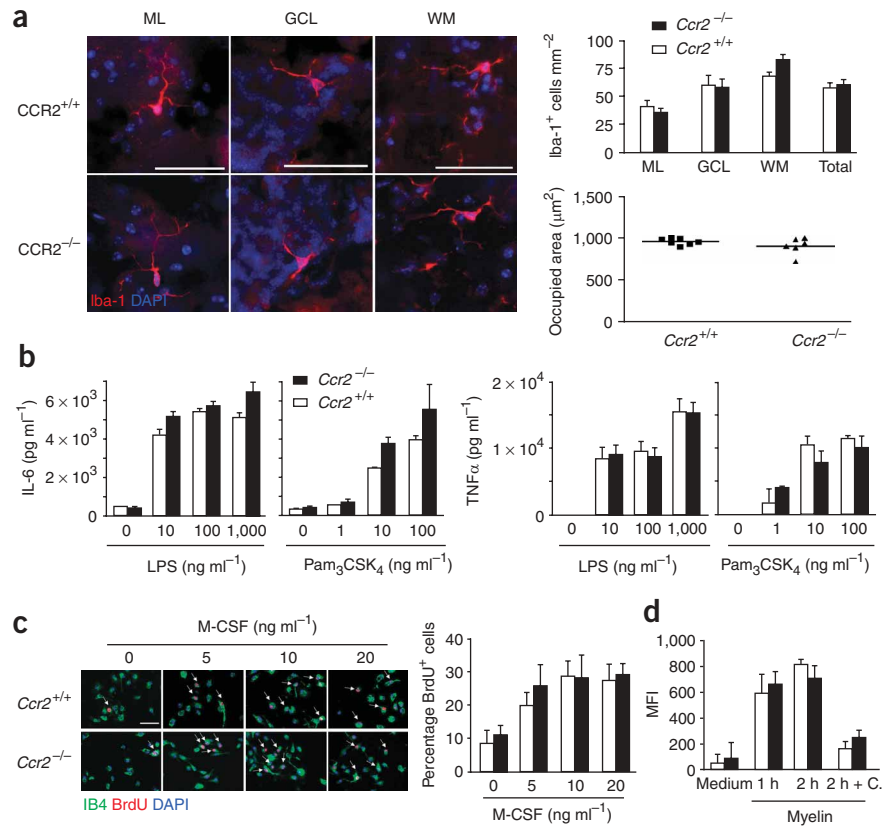
CCR2-independent development and function of microglia

Because the chemokine receptor CCR2 is crucial for monocyte and macrophage function (for example, for the chemotactic attraction during inflammation²⁶), we investigated a potential role for CCR2 in the development and immunological properties of microglia. Morphology of brain microglia in the absence of CCR2 was assessed by using immunofluorescence staining with the macrophage and microglia marker Iba-1 (red, Fig. 2a). In different regions of the cerebellum (molecular layer, granular cell layer and white matter), Iba-1⁺ parenchymal cells with typical round to spindle-shaped microglial morphology and distinct arborization pattern were undistinguishable in *Ccr2*^{+/+} and *Ccr2*^{-/-} brains (Fig. 2a, left). Quantitative morphometric analysis revealed comparable numbers of parenchymal Iba-1⁺ microglia in different regions of the cerebellum. Cell dimension, as judged by the microglia occupying area ($908 \pm 40 \mu\text{m}^2$ in *Ccr2*^{-/-} and $957 \pm 14 \mu\text{m}^2$ in *Ccr2*^{+/+}), was similar irrespective of the genotype (Fig. 2a, right).

We next examined the microglial ability to respond to the Toll-like receptors 2 and 4 ligands, lipopolysaccharide (LPS) and the lipopeptide Pam₃CSK₄, in a dose-dependent manner (Fig. 2b). Both CCR2-deficient and competent microglia produced similar amounts of the proinflammatory cytokines interleukin 6 (IL-6) and tumor

Figure 2 Normal development, morphology and function of microglia in the absence of CCR2. (a) Iba-1 immunohistochemistry (red) and DAPI staining of nuclei (blue) of cerebellar sections from 8-week-old *Ccr2*^{+/+} and *Ccr2*^{-/-} mice revealed the same morphology and arborization pattern of parenchymal microglia in the molecular layer (ML), granule cell layer (GCL) and in the white matter (WM, upper left). Scale bars represent 40 μ m. The same number of Iba-1⁺ ramified parenchymal cells was found in different localizations of the cerebellum (upper right). Data are expressed as means \pm s.e.m. At least eight mice were examined for each group. Iba-1⁻ immunoreactive areas in the cerebellar WM were quantified by determining the areas covered by the outer-most cell processes (lower right). For each mouse, at least 25 cells were assessed quantitatively. Each symbol represents the mean measurements in one mouse. The mean is indicated for each group. (b) Unaltered cytokine response in *Ccr2*^{-/-} microglia. *Ccr2*^{+/+} (white bars) or *Ccr2*^{-/-} microglia (black bars) were exposed to increasing dosages of either LPS or Pam₃CSK₄, and production of TNF α and IL-6 was measured by ELISA 18 h after exposition. Data represent means \pm s.e.m. of three independent experiments. No statistically significant differences were detected ($P > 0.05$).

(c) Microglia cell proliferation does not require CCR2. Primary microglia were treated with different concentrations of M-CSF for 48 h. We added 10 μ M BrdU for 1 h and the cells were stained for isolectin B4 (green), BrdU (red) and DAPI (blue). Representative images are shown in the left panel. Scale bar represents 50 μ m. Quantification of the percentage of BrdU⁺ microglia revealed no differences in the proliferative responses of *Ccr2*^{+/+} (white bars) or *Ccr2*^{-/-} (black bars) microglia to M-CSF. (d) Mean fluorescence intensities (MFI) of *Ccr2*^{+/+} (white bars) and *Ccr2*^{-/-} (black bars) microglia ingesting fluorescein isothiocyanate-labeled myelin after 1 h, 2 h or after exposure of myelin with cytochalasin D for 2 h (+ C). Data represent means \pm s.e.m. of three independent experiments.



necrosis factor α (TNF α) after ligand challenge. In addition, surface expression of MHC class II molecules was upregulated to a similar degree after interferon γ (IFN γ) stimulation (**Supplementary Fig. 1** online). Recombinant IFN β , in turn, counteracted the IFN γ -induced MHC class II expression levels to a similar extent in *Ccr2*^{+/+} and *Ccr2*^{-/-} primary microglia. Because CCR2 may not only affect the activation response, we also investigated the effect of CCR2 on microglia proliferation (**Fig. 2c**). No difference was found in the ability of macrophage colony-stimulating factor (M-CSF) to stimulate microglia proliferation in the presence or absence of CCR2. We next exposed cultured microglia to fluorescently labeled myelin and measured the kinetics and quantity of myelin phagocytosis (**Fig. 2d**). Myelin uptake by microglia was independent of CCR2 expression, and could be specifically inhibited by incubation with cytochalasin D. Taken together, our data indicate that microglial development, morphology and innate immune functions are preserved in the absence of CCR2.

Postnatal microglia derive from Ly-6C^{hi}CCR2⁺ monocytes

As a result of the strong and specific reduction of the Ly-6C^{hi} subpopulation in the absence of CCR2, *Ccr2*^{-/-} mice are a suitable tool for determining the monocyte fraction that might be the direct precursor of adult microglia in the peripheral blood. To do so, we generated double-transgenic mice by intercrossing ACT β (β -actin)-EGFP mice with *Ccr2*^{-/-} mice. These mice express GFP on the *Ccr2*^{+/+} (*Ccr2*^{+/+}GFP) or the *Ccr2*^{-/-} (*Ccr2*^{-/-}GFP) background, respectively. To distinguish invading bone marrow-derived monocytes

from brain endogenous microglia during health and disease, we created bone-marrow chimeras. Respective GFP-marked BMCs were mixed with unlabeled WT BMCs (at a 1:3 ratio) and transplanted into lethally whole-body irradiated (including the brain) adult recipient mice. In the resulting *Ccr2*^{+/+}GFP \rightarrow *Ccr2*^{+/+} chimeras (*Ccr2*^{+/+}Ch), both monocyte subsets express GFP, whereas chimeric *Ccr2*^{-/-}GFP \rightarrow *Ccr2*^{+/+} mice (*Ccr2*^{-/-}Ch) express the fluorophore predominantly on Ly-6C^{lo} monocytes. As expected, peripheral blood Gr-1^{hi} (Ly-6C^{hi}) monocytes were strongly diminished in chimeric *Ccr2*^{-/-}Ch mice compared with *Ccr2*^{+/+}Ch mice 4 weeks after bone-marrow transfer (exemplified in **Fig. 3a**). The general reconstitution efficacy, however, was similar in *Ccr2*^{-/-}Ch and *Ccr2*^{+/+}Ch mice, as indicated by comparable numbers of GFP⁺CD3⁺ and GFP⁺B220⁺ lymphocytes (**Fig. 3b**).

To assess the ability of GFP-marked monocyte subsets derived from transplanted bone marrow to differentiate into microglia in the nondiseased brain, we analyzed recipient mice histologically 12 weeks after transplantation (**Fig. 3c–e**). Microscopical investigation of several CNS regions, such as the cerebellum, brain stem (**Fig. 3c**) and spinal cord (**Fig. 3e**), revealed some parenchymal cells with typical microglial morphology. These donor-derived GFP⁺ cells were Iba-1⁺ (**Fig. 3c,e**), as well as for the pan-macrophage marker F4/80 (**Fig. 3d**). Moreover, the engrafted cells were MHC class II⁻ and were CD45^{lo}, as determined by fluorescent-activated cells sorting (FACS) analysis (data not shown), providing further evidence for their microglial identity. Notably, however, engrafted GFP⁺Iba-1⁺ cells were predominantly found in the CNS of *Ccr2*^{+/+}Ch mice, whereas the number of engrafted microglia

in $Ccr2^{-/-Ch}$ mice specifically lacking $Ly-6C^{hi}$ monocytes was greatly reduced in the molecular layer of the cerebellum (for example, 1.4 ± 0.3 cells mm^{-2} in $Ccr2^{+/+Ch}$ mice and no detectable $GFP^{+}Iba-1^{+}$ cells in $Ccr2^{-/-Ch}$ mice) and in the spinal cord white matter (2.8 ± 1.0 cells mm^{-2} in $Ccr2^{+/+Ch}$ mice and no detectable cells in $Ccr2^{-/-Ch}$ mice).

In conclusion, our data strongly suggest that $Ly-6C^{hi}CCR2^{+}$ monocytes are the main source of bone marrow-derived microglia in several regions of the healthy adult CNS in a standard chimeric experimental setup that comprises irradiation of the CNS before bone-marrow reconstitution.

Host factors modulate microglia engraftment during health

The possibility that whole-body irradiation conditions the brain to microglia engraftment has been rarely addressed experimentally in

previous studies^{7,8,27}. We therefore adapted the protocol using linear acceleration irradiation, which allows targeted irradiation that includes or excludes the brain before bone-marrow transplantation. As an obvious macroscopical sign of radiation protection, C57BL/6 mice that received selective-body irradiation (omitting the brain) retained the black fur color only on the head at 12 weeks after bone-marrow transplantation (Fig. 4a). These mice are subsequently referred to as 'protected' mice, in contrast to the 'unprotected' ones. It has been reported that irradiation of the CNS induces a tremendous and rapid gene regulation^{28,29}. We therefore measured the time-dependent induction of several myeloattractants and $TNF\alpha$ in irradiated unprotected and nonirradiated protected parts of the CNS (Fig. 4b). Notably, we observed a strong induction of cytokines and chemokines at 16 d after irradiation in the unprotected spinal cord, but not in the nonexposed

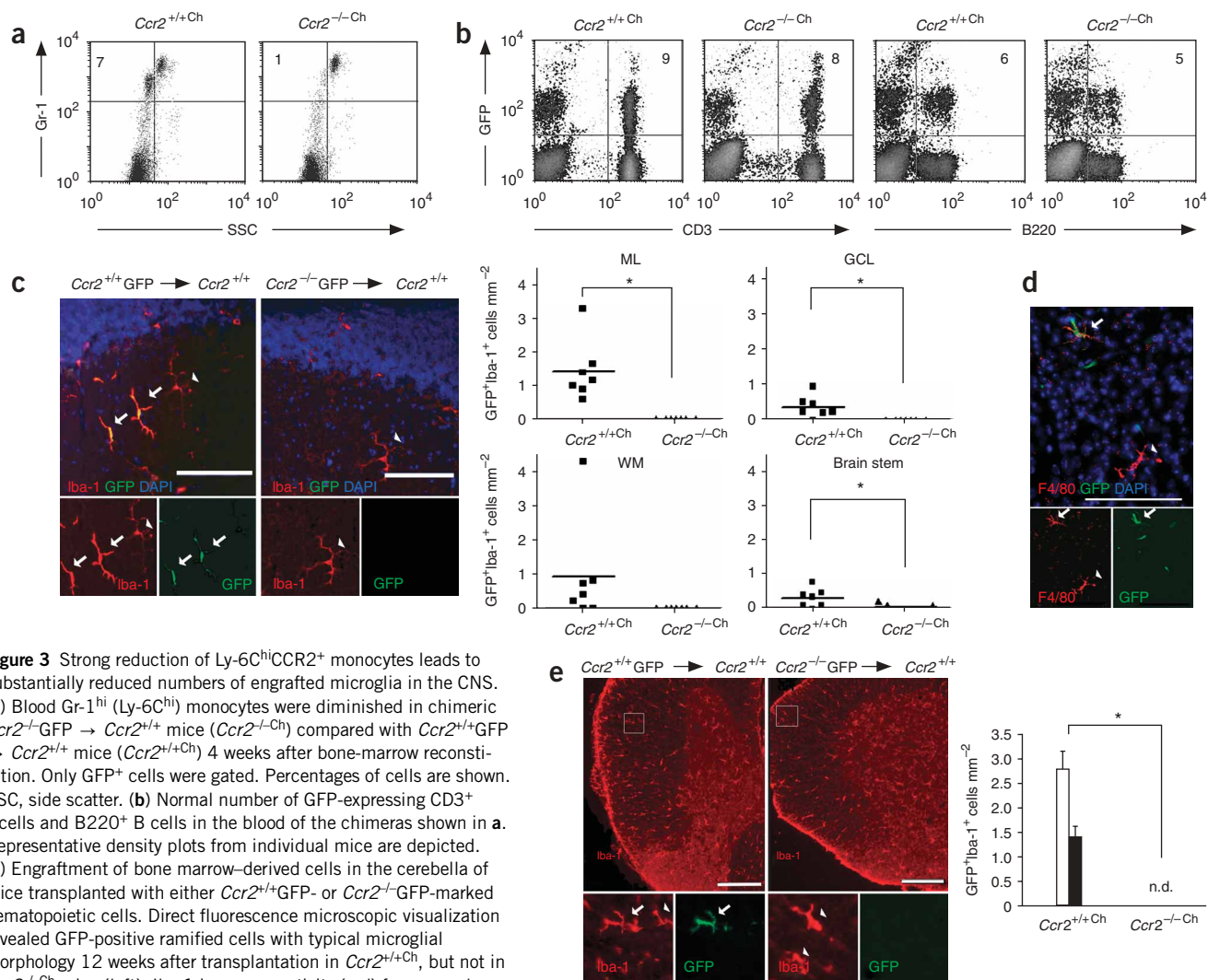


Figure 3 Strong reduction of $Ly-6C^{hi}CCR2^{+}$ monocytes leads to substantially reduced numbers of engrafted microglia in the CNS.

(a) Blood $Gr-1^{hi}$ ($Ly-6C^{hi}$) monocytes were diminished in chimeric $Ccr2^{-/-}GFP \rightarrow Ccr2^{+/+}$ mice ($Ccr2^{-/-Ch}$) compared with $Ccr2^{+/+}GFP \rightarrow Ccr2^{+/+}$ mice ($Ccr2^{+/+Ch}$) 4 weeks after bone-marrow reconstitution. Only GFP^{+} cells were gated. Percentages of cells are shown. SSC, side scatter. (b) Normal number of GFP -expressing $CD3^{+}$ T cells and $B220^{+}$ B cells in the blood of the chimeras shown in a. Representative density plots from individual mice are depicted.

(c) Engraftment of bone marrow-derived cells in the cerebella of hematopoietically transplanted with either $Ccr2^{+/+}GFP$ - or $Ccr2^{-/-}GFP$ -marked hematopoietic cells. Direct fluorescence microscopic visualization revealed GFP -positive ramified cells with typical microglial morphology 12 weeks after transplantation in $Ccr2^{+/+Ch}$, but not in $Ccr2^{-/-Ch}$ mice (left). $Iba-1$ immunoreactivity (red) for macrophages and microglia showed that some branched cells are GFP^{+} and are therefore of hematopoietic origin (GFP , green, arrows), whereas others represent endogenous microglia expressing $Iba-1$ only (arrowheads). Scale bars represent 70 μm (overviews) and 25 μm (inserts). Semi-quantitative analysis of regional microglia engraftment ($GFP^{+}Iba-1^{+}$ cells) in the ML, GCL, WM and the brain stem 12 weeks after reconstitution (right). Each symbol indicates the value obtained per region from at least three sections in individual mice. Asterisks highlight statistical significances ($P < 0.05$).

(d) Donor-derived GFP^{+} cells expressed the macrophage marker $F4/80$ (arrows). Some brain-endogenous microglia also showed $F4/80$ immunoreactivity (arrowheads). Scale bar represents 25 μm . (e) GFP^{+} ramified cells were detected in the spinal cords of $Ccr2^{+/+Ch}$, but not of $Ccr2^{-/-Ch}$ mice. Blood-derived cells were mostly $Iba-1^{+}$ (arrow), whereas radio-resistant host microglia expressed $Iba-1$ only (arrowheads). Scale bars represent 200 μm . Quantitative assessment (right) revealed significantly more $GFP^{+}Iba-1^{+}$ cells in the gray matter (GM, black bar) and WM (white bar) if the donor BMCs are $Ccr2^{+/+}GFP$ ($Ccr2^{+/+Ch}$) ($P < 0.05$). Data represent means \pm s.e.m. n.d., not detectable. Representative photographs are shown. For quantification, at least 3 sections of lumbar, thoracic and cervical spinal cords segments from 7–8 mice per group were used.

protected brain tissue (8.0 ± 3.4 versus 2.4 ± 0.2 -fold increase for CXCL10, $P = 0.09$; 8.7 ± 2.1 versus 0.7 ± 0.2 -fold increase for CXCL10, $P = 0.002$; 3.6 ± 0.7 versus 0.7 ± 0.3 -fold increase for CCL2, $P = 0.04$; 4.0 ± 0.7 versus 0.6 ± 0.1 -fold increase for TNF α , $P = 0.003$). This significant chemokine and cytokine increase after 16 d appears to coincide with the appearance of GFP-expressing cells in perivascular and leptomeningeal sites at 2 weeks after bone-marrow transplantation⁸. To address the question of whether this chemokine induction might promote the selective engraftment of Ly-6C^{hi}CCR2⁺ monocytes in the irradiated parts of the CNS, we examined brain sections from the chimeric mice histologically (Fig. 4c). Notably, CNS microglia engraftment occurred only in regions of the brain that were conditioned by irradiation. Thus, significant numbers of GFP⁺Iba-1⁺-grafted microglia could only be detected in the spinal cord of *Ccr2*^{+/+Ch} mice, which still contained the Ly-6C^{hi} population in the blood (2.9 ± 0.9 GFP⁺Iba-1⁺ cells mm⁻² in *Ccr2*^{+/+Ch} mice compared with no GFP⁺Iba-1⁺ cells in *Ccr2*^{-/-Ch} chimeras, $P = 0.04$). The protected brains of either *Ccr2*^{+/+Ch} or *Ccr2*^{-/-Ch} mice, however, did not show any donor-derived microglia in the cerebellum (Fig. 4c) or in the other regions examined, such as the cortex, striatum and hippocampus (data not shown).

Another possibility of hematopoietic reconstitution with donor-derived blood cell progeny without irradiation is the use of the *Rag2*^{-/-} \times γ_c ^{-/-} mice as recipients. Successful and stable lymphoid and myeloid reconstitution was achieved in *Rag2*^{-/-} \times γ_c ^{-/-} mice 32 weeks after BMC transfer (Fig. 4d). The number of GFP⁺B220⁺ lymphoid cells was similar in both *Ccr2*^{-/-Ch} \rightarrow *Rag2*^{-/-} \times γ_c ^{-/-} chimeric mice (*Ccr2*^{-/-Ch}) and *Ccr2*^{+/+Ch} \rightarrow *Rag2*^{-/-} \times γ_c ^{-/-} mice (*Ccr2*^{+/+Ch}) (Fig. 4d, upper left). As expected, the amount of Gr-1⁺ (Ly-6C^{hi}) cells was strongly reduced in the blood of *Ccr2*^{-/-Ch} mice (Fig. 4d, upper right). Subsequent histological examination of the brains from *Ccr2*^{-/-Ch} and *Ccr2*^{+/+Ch} mice revealed donor-derived Iba-1-expressing perivascular cells, but no GFP⁺Iba-1⁺ ramified microglia in the cerebellar parenchyma (Fig. 4d, lower row). Single bipolar GFP⁺Iba-1⁻ cells with immature morphology were rarely detected in the *Ccr2*^{-/-Ch} cerebella (Fig. 4d, lower left).

In summary, our data provide strong evidence that microglia engraftment requires conditioning of the nondiseased adult CNS (as in our case, irradiation). Gene therapy protocols without CNS conditioning might fail to attract sufficient bone marrow-derived Ly-6C^{hi} cells to the brain.

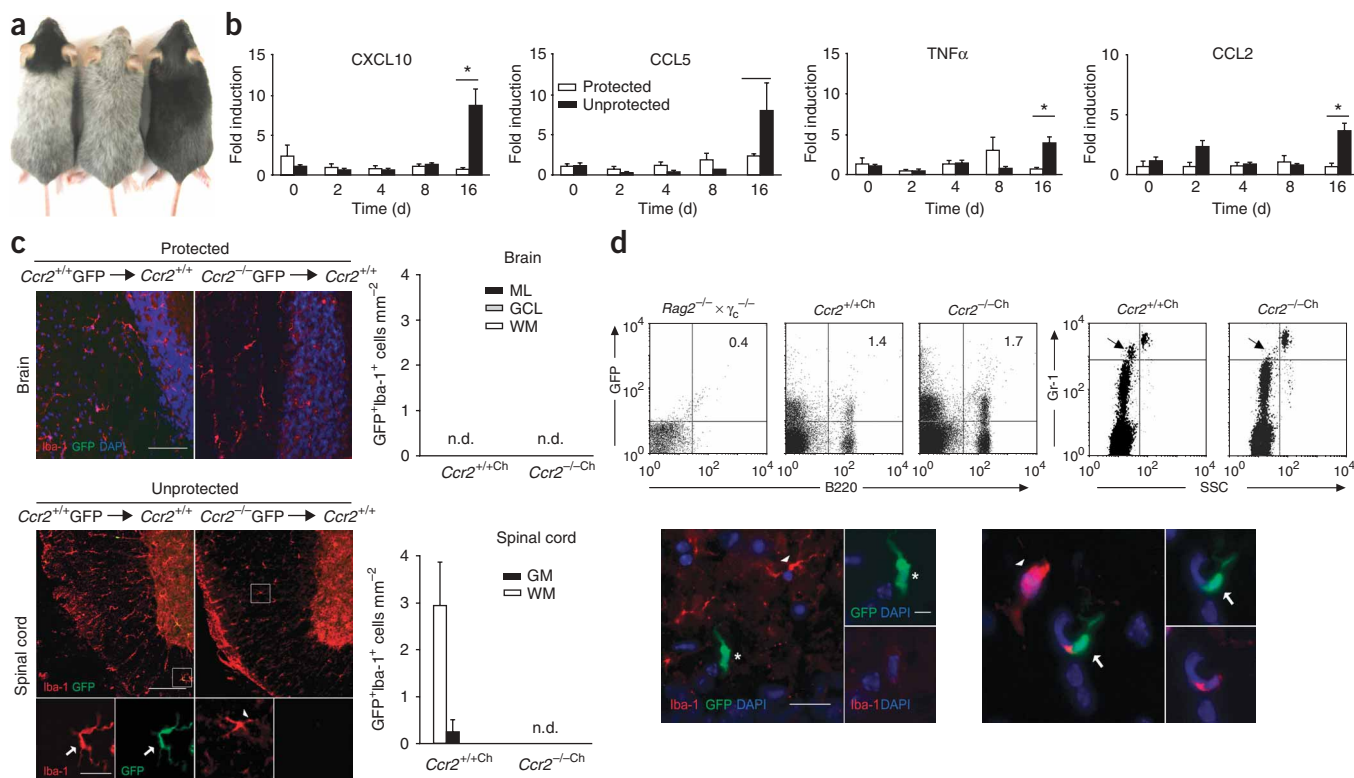


Figure 4 Engraftment of donor-derived GFP⁺Ly-6C^{hi}CCR2⁺ monocytes and differentiation into microglia requires a conditioned CNS. (a) Photograph showing long-term change of fur color. Irradiation led to selective loss of black fur color in the irradiated areas beginning at 3 months after irradiation, whereas the nonexposed head fur was unaffected. Left, protected mouse; middle, unprotected mouse; right, nonirradiated mouse. (b) Quantitative real-time PCR analysis of cytokine and chemokine induction in irradiated unprotected segments (lumbar spinal cord, black columns) and nonirradiated protected parts (brain, white bars) of the CNS after indicated time points post-irradiation. Data are means \pm s.e.m. Asterisks indicate statistical significance. (c) Engraftment of donor-derived GFP⁺ ramified cells in the CNS parenchyma 12 weeks after transplantation occurred only if the region was previously irradiated (unprotected) and had a CCR2⁺ genotype (*Ccr2*^{+/+Ch}, left panel). Arrows label bone marrow-derived GFP⁺Iba-1⁺ cells and arrow heads mark endogenous host Iba-1⁺ microglia. Scale bars represent 25 μ m (brain) or 200 μ m (spinal cord, overview), and 25 μ m (spinal cord, insert). Quantification of microglia engraftment is shown on the right. At least seven mice per group were used for quantification. (d) Successful lymphoid (B220) and myeloid (Gr-1) reconstitution in nonirradiated *Rag2*^{-/-} \times γ_c ^{-/-} mice 32 weeks after transfer of BMCs. *Ccr2*^{-/-Ch} \rightarrow *Rag2*^{-/-} \times γ_c ^{-/-} chimeric mice (*Ccr2*^{-/-Ch}) had a reduced number of Ly-6C^{hi} (Gr-1⁺) monocytes in the peripheral blood (upper row, percentages are shown). Only GFP⁺ cells were gated. Identification of donor-derived cells in the brains of chimeric mice 3 months after transplantation revealed no GFP⁺Iba-1⁺ ramified parenchymal cells in the host cerebella (lower). Endogenous microglia are Iba-1⁺ (arrowheads). There was a single elongated bipolar cell having no typical microglia-like morphology that was GFP⁺Iba-1⁻ (asterisk, lower left). Occasionally, GFP⁺Iba-1⁺ perivascular cells were found 3 months after bone-marrow transfer (arrow, lower right). Scale bars represent 25 μ m (overview) and 5 μ m (insert).

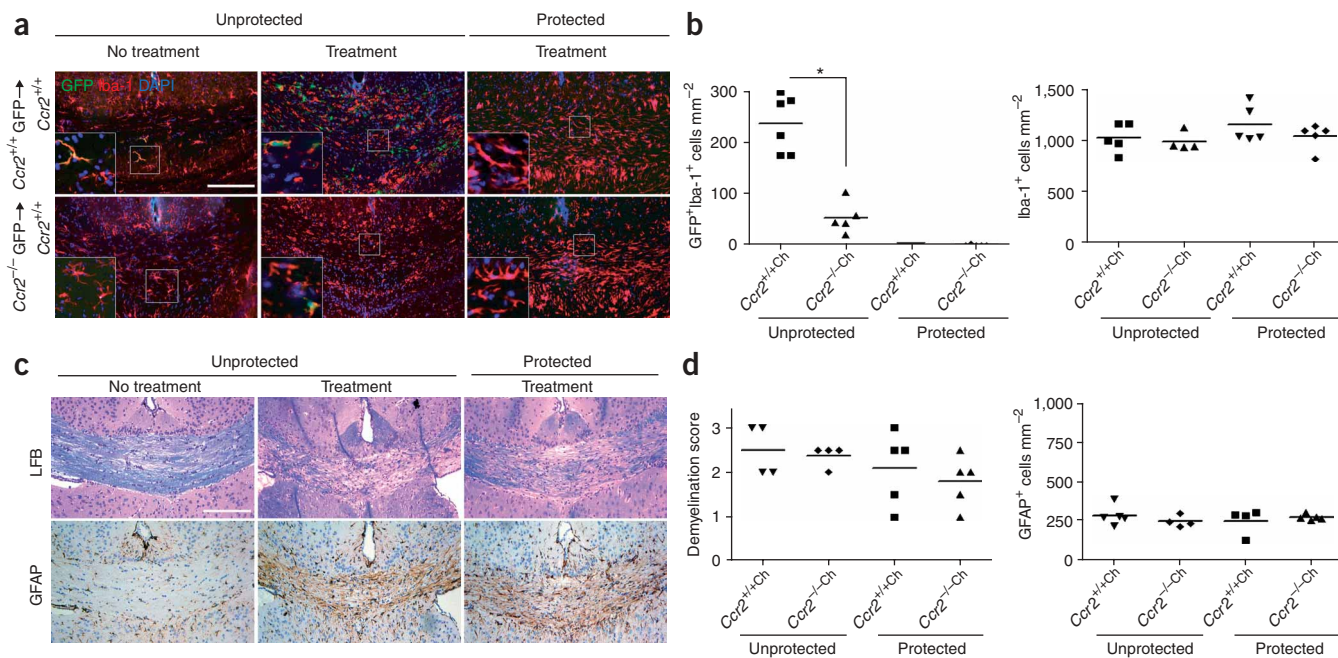


Figure 5 Immigration of Ly-6^{Ch} monocytes into the brain during cuprizone-induced demyelination requires host conditioning. **(a)** Engraftment of bone marrow-derived GFP⁺ cells in the corpus callosum of brain-irradiated (unprotected) or non-brain-irradiated (protected) *Ccr2*^{+/+}GFP → *Ccr2*^{+/+} (*Ccr2*^{+/+}Ch) and *Ccr2*^{-/-}GFP → *Ccr2*^{+/+} (*Ccr2*^{-/-}Ch) chimeric mice after 5 weeks of cuprizone treatment (treated) or in untreated mice. Arrows point to double-positive GFP⁺Iba-1⁺ blood-derived cells, whereas arrowheads indicate radio-resistant Iba-1⁺ host microglia. Scale bar represents 200 μm. **(b)** Quantitative assessment of donor-derived GFP⁺Iba-1⁺ macrophages and microglia (left) and overall Iba-1⁺ cells (right) in the corpus callosum of chimeric mice 5 weeks after cuprizone treatment. Each symbol corresponds to the mean of one mouse after evaluation of at least two tissue sections. The mean is indicated for each group. **(c,d)** The extent of demyelination was evaluated qualitatively **(c)** and semi-quantitatively **(d)** by LFB staining and by immunohistochemistry for the astrocyte marker GFAP. Scale bar represents 200 μm. Representative microphotographs are shown. In the quantitative analysis, each symbol represents the mean from at least three tissue sections derived from one individual mouse. The mean is indicated for each group. No statistically significant differences were found ($P > 0.05$).

No frank microglia engraftment during CNS neuropathology

To investigate whether the generation of microglia from Ly-6^{Ch}CCR2⁺ monocytes is enhanced during CNS pathology and whether microglia recruitment into the diseased brain also requires a favorable host environment, we induced (i) demyelination in adult mice using the copper chelator cuprizone as a model of primary demyelination and (ii) neurodegeneration in adult mice using the facial nerve axotomy model.

Treatment with cuprizone, administered as a food additive, induces demyelination selectively in the corpus callosum. Notably, cuprizone-induced demyelination does not promote blood-brain barrier damage^{30,31}, but recruitment of peripheral macrophages has been reported in irradiated bone-marrow chimeric mice³².

Following bone-marrow transfer, protected and unprotected *Ccr2*^{+/+}GFP → *Ccr2*^{+/+} (*Ccr2*^{+/+}Ch) and *Ccr2*^{-/-}GFP → *Ccr2*^{+/+} (*Ccr2*^{-/-}Ch) chimeric mice were challenged with cuprizone, and microglia engraftment during toxic demyelination was investigated (**Fig. 5**). In unprotected mice, numerous Iba-1⁺ GFP-expressing cells selectively infiltrated the demyelinated corpus callosum. However, the extent of engraftment appeared to be markedly more extensive in unprotected *Ccr2*^{+/+}Ch mice compared with unprotected *Ccr2*^{-/-}Ch mice (**Fig. 5a**). Both endogenous GFP-Iba-1⁺ and engrafted GFP-Iba-1⁺ macrophages and microglia showed morphological signs of activation, namely retraction of processes and rounding of cell soma. Quantification of donor-derived GFP⁺Iba-1⁺ macrophage and microglia engraftment revealed significantly more cells in the unprotected *Ccr2*^{+/+}Ch group as compared with unprotected *Ccr2*^{-/-}Ch mice (236.5 ± 55.5 GFP⁺Iba-1⁺ cells mm⁻² in unprotected *Ccr2*^{+/+}Ch mice, 54.0 ± 30.6 cells mm⁻² cells

in unprotected *Ccr2*^{-/-}Ch chimeras, $P < 0.001$), indicating that Ly-6^{Ch}CCR2⁺ monocytes were recruited to the demyelinating lesion in the irradiated brain (**Fig. 5b**, left). The few GFP⁺Iba-1⁺ cells found in the corpus callosum of *Ccr2*^{-/-}Ch chimeras most likely represent descendants of the residual Ly-6^{Ch} cells found in the peripheral blood of these mice. No GFP⁺Iba-1⁺ cells were detectable in the protected groups, irrespective of the genotype of the donor bone marrow. The data indicate that Ly-6^{Ch} monocytes are only recruited to the demyelinating lesion when the brain was irradiated. Notably, the overall number of Iba-1⁺ cells was not substantially different in any of the chimeric groups investigated (**Fig. 5b**, right). We observed a strong local production of CCL2, CXCL10, CCL5 and TNFα in the damaged corpus callosum of WT mice after 5 weeks of cuprizone treatment (**Supplementary Fig. 2** online), which was obviously not sufficient to trigger monocyte entry across the intact blood-brain barrier. To evaluate the contribution of donor-derived Ly-6^{Ch}CCR2⁺ monocytes to the process of demyelination, we evaluated the loss of myelin semi-quantitatively by luxol fast blue (LFB) staining (**Fig. 5c,d**). Demyelination was extensive in all experimental groups, with no statistically significant differences ($P > 0.1$). The distribution and amount of reactive GFAP⁺ astrocytes were indistinguishable between the experimental groups (**Fig. 5d**, right).

To exclude the possibility that CCR2-knockout mice show effects from the genetic manipulation that are independent of CCR2 deficiency, we also carried out adoptive transfer experiments. We took advantage of the α-CCR2 antibody MC-21, which selectively depletes Ly-6^{Ch} CCR2⁺, but not Ly-6^{Ch} CCR2⁻ monocytes in the peripheral blood (**Fig. 6a**) by an antibody-dependent cellular

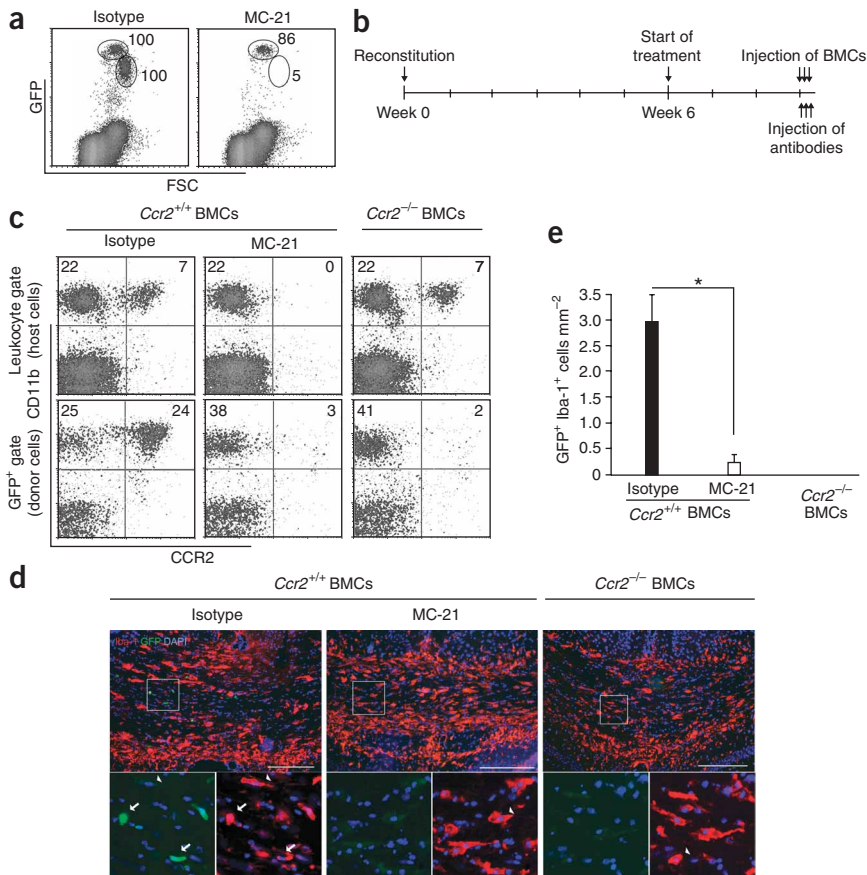


Figure 6 Adoptively transferred Ly-6C^{hi}CCR2⁺ monocytes selectively migrate to the demyelinated area in the conditioned CNS. **(a)** MC-21 specifically depletes GFP^{lo} monocytes (Ly-6C^{hi}CCR2⁺), but only barely affects GFP^{hi} monocytes (Ly-6C^{lo}CCR2⁻) in CX₃CR1^{GFP/+} mice. **(b)** Time scale of Ly-6C^{hi}CCR2⁺ depletion experiments using MC-21 in cuprizone-challenged chimeric mice (*Ccr2*^{+/+} → *Ccr2*^{+/+}). **(c)** FACS analysis revealed the depletion of CCR2⁺ host cells (upper middle), as well as of adoptively transferred GFP⁺CCR2⁺ donor cells (lower middle), in the chimeric mice after injection of MC-21 versus isotype control injection (left). CCR2 expression could not be detected in the group receiving GFP⁺CCR2⁻ BMCs (right). **(d,e)** Engraftment of donor-derived GFP⁺Iba-1⁺ macrophages in the lesioned brain occurred when adoptively transferred GFP⁺CD11b⁺CCR2⁺ BMCs were treated with the isotype control, but not when these cells were depleted by MC-21 or when CCR2⁻ BMCs were used. Immunohistochemistry of brains 4 weeks after cuprizone challenge is shown **(d)**. Arrows point to double-positive GFP⁺Iba-1⁺ blood-derived cells, whereas arrowheads indicate radio-resistant Iba-1⁺ host microglia. Scale bars represent 200 μm. Quantitative assessment of donor-derived GFP⁺Iba-1⁺ monocytes in the corpus callosum of chimeric mice 5 weeks after cuprizone treatment **(e)**. Data are means ± s.e.m. Asterisk indicates statistically significant difference (*P* < 0.05). At least four mice per group were examined.

cytotoxicity-mediated mechanism (data not shown). BMCs were injected intravenously into irradiated cuprizone-treated chimeric mice (*Ccr2*^{+/+} → *Ccr2*^{+/+}), and Ly-6C^{hi}CCR2⁺ cells were subsequently depleted (Fig. 6b). Immunohistochemical analysis revealed that donor-derived GFP⁺Iba-1⁺ monocytes were only recruited to areas of demyelination when the Ly-6C^{hi}CCR2⁺ subpopulation was present in the blood (Fig. 6c–e). Notably, we found that adoptively transferred *Ccr2*^{-/-}Ly-6C^{hi} monocytes could not be detected in the corpus callosum of cuprizone-treated mice. These data suggest that CCR2-dependent chemotaxis is a necessary process for monocytes to enter the lesioned and conditioned brain.

Finally, protected and unprotected CCR2-chimeras were subjected to unilateral facial nerve axotomy (Fig. 7). In this experimental procedure, the blood-brain barrier is intact, and a remote degeneration of the facial nucleus leads to local microglial activation with concomitant recruitment of bone marrow-derived microglia in whole-body irradiated mice⁸. Ramified GFP-expressing cells were found in close proximity to the lesioned facial motoneurons in unprotected *Ccr2*^{+/+}GFP → *Ccr2*^{+/+} (*Ccr2*^{+/+Ch}) mice 14 d after axotomy, and to a lesser degree in unprotected *Ccr2*^{-/-}GFP → *Ccr2*^{+/+} (*Ccr2*^{-/-Ch}) mice (Fig. 7a,c). These cells were identified as microglia by their morphology and by the expression of the Iba-1 antigen. In contrast, the unlesioned contralateral facial nucleus was largely devoid of engrafted GFP⁺ microglia. Again, selective recruitment of donor-derived BMCs to the side of neurodegeneration took place only when the brain was primed before by irradiation. We found significantly more ramified GFP⁺Iba-1⁺ cells in the lesioned facial nucleus of *Ccr2*^{+/+Ch} mice (94.1 ± 2.5 GFP⁺Iba-1⁺ cells mm⁻²) than in *Ccr2*^{-/-Ch} mice (38.3 ± 3.2 cells mm⁻²) (*P* < 0.001). As expected, no ramified GFP-expressing cells

were found in the lesioned facial nuclei of protected *Ccr2*^{+/+Ch} mice and protected *Ccr2*^{-/-Ch} mice (Fig. 7b,c). These results underscore the requirement of brain conditioning for efficient microglia engraftment from circulating Ly-6C^{hi} monocytes in CNS diseases with intact blood-brain barriers.

DISCUSSION

In this study, we identified a specific monocyte subpopulation, namely Ly-6C^{hi}Gr-1⁺CCR2⁺CX₃CR1^{lo} cells, as the precursor of adult murine microglia in the peripheral blood. Ly-6C^{hi} CCR2⁺ monocytes specifically accumulated in CNS lesions and differentiated into brain-specific macrophages, the microglia. Furthermore, we found that microglia engraftment during postnatal life is enhanced by CNS pathology, but requires conditioning of the brain (for example, by irradiation) if the blood-brain barrier remains intact. Thus, our data offer new insights into the mechanisms leading to microglia engraftment in the adult brain under normal and diseased conditions, and suggest a role for specific monocyte subpopulations as direct circulating microglia precursors.

The first microglia colonization of the CNS takes place during early embryogenesis, when microglia arise from hemangioblastic mesoderm and populate the developing neuroectoderm in rodents after embryonic day 8.5 (ref. 33). This early microglia engraftment most likely occurs independently of CCR2, as we could not detect any changes in the number, distribution, morphology or innate immune function of Iba-1⁺ microglia in *Ccr2*^{-/-} mice. During embryogenesis, microglia development is thought to be orchestrated by factors of the early myelopoiesis, such as PU.1 or M-CSF³⁴. Notably, parenchymal microglia can arise from BMCs in nonirradiated neonates³⁵, demonstrating that our findings are specific for the adult CNS. The

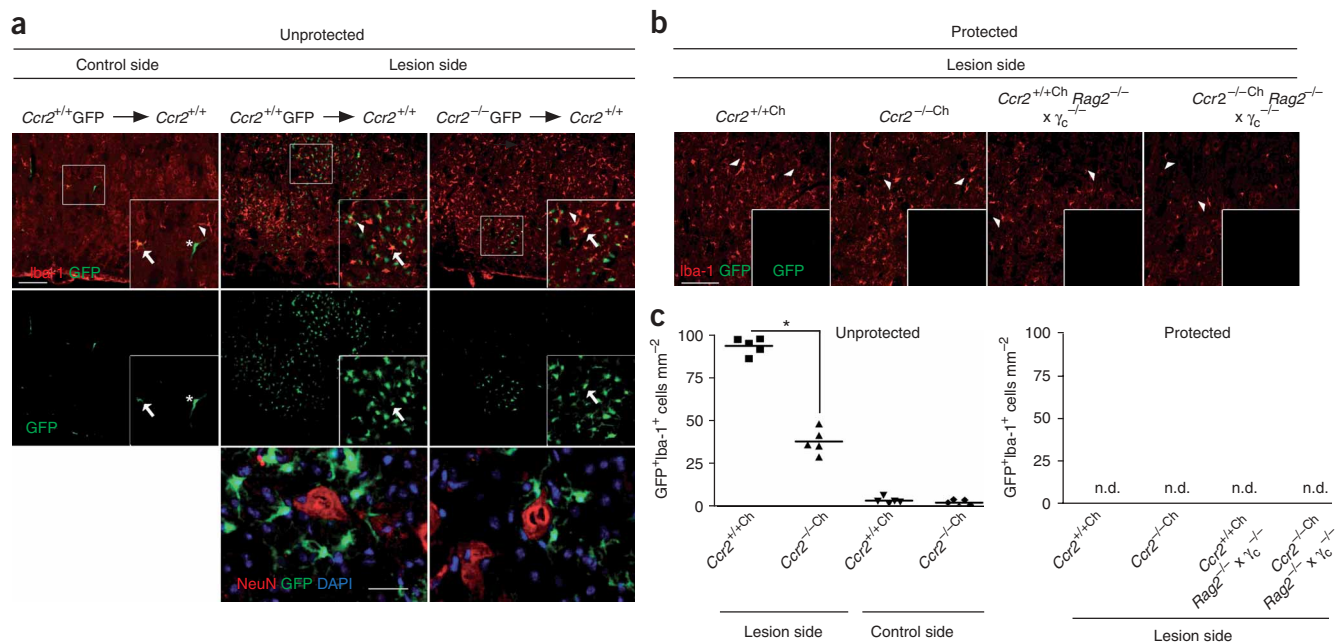


Figure 7 Selective recruitment of donor-derived Ly-6C^{hi}CCR2⁺ monocytes after axotomized facial nucleus occurs only in conditioned CNS. **(a, b)** Microglia engraftment in the lesioned facial nucleus following facial nerve axotomy. Ramified GFP-expressing cells 14 d after axotomy express Iba-1 (arrows). Endogenous host microglia are Iba-1⁺ (arrowheads). **(a)** In the unprotected control (nonlesioned) facial nucleus, one GFP⁺ bipolar cell without microglia characteristics (asterisk). More numerous GFP-positive ramified cells were found in the lesioned facial nucleus of $Ccr2^{+/+}GFP \rightarrow Ccr2^{+/+}$ ($Ccr2^{+/+}Ch$) mice than $Ccr2^{-/-}GFP \rightarrow Ccr2^{+/+}$ ($Ccr2^{-/-}Ch$) chimeric mice. Scale bar represents 100 μ m (upper and middle). Some ramified GFP-expressing cells were in close proximity to NeuN-immunoreactive neurons (red) in the facial nucleus in $Ccr2^{-/-}Ch$ chimeras (lower). Scale bar represents 10 μ m. DAPI staining is shown in blue. **(b)** No engraftment of GFP⁺ cells was found in the nonirradiated (protected) chimeras of any genotype. Iba-1 immunoreactivity identified host microglia (arrowheads). Scale bar represents 100 μ m. **(c)** Quantification of donor-derived microglia and macrophage engraftment (GFP⁺Iba-1⁺) in the lesioned facial nucleus or the contralateral control facial nucleus 14 d after axotomy. A robust engraftment of GFP⁺Iba-1⁺ cells was found only in brain-irradiated (unprotected) $Ccr2^{+/+}Ch$ mice, whereas significantly fewer engrafted cells were visible in $Ccr2^{-/-}Ch$ chimeric mice lacking Ly-6C^{hi} monocytes ($P < 0.001$). Irradiation-protected mice failed to show any engrafted GFP⁺ cells in the facial nucleus. Symbols indicate individual mice. For all experimental groups, five mice were used. Asterisk shows statistically significant difference ($P < 0.05$).

generation of microglia in the adult brain, however, is still a matter of debate. Initial studies using lethally irradiated rats found only limited turnover of microglia with their peripheral myeloid counterparts in the blood, which might be, at least in part, explained by the technical limitations of using MHC mismatch as a marker of donor BMCs⁷. More recently, labeling methods of BMCs, such as retroviral and transgenic approaches, have facilitated tracking of bone marrow-derived cells and their differentiation in the brain. A high percentage of newly engrafted microglia was observed in the adult mouse brain using this technique⁸. These initial data were confirmed and extended by others^{17,36,37}. Even therapeutic approaches were successfully established using genetically modified microglia precursors in the blood as cellular vehicles for CNS gene therapy of metachromatic leukodystrophy in whole body-irradiated chimeras³⁸.

Further studies documented an early and rapid engraftment of bone marrow-derived microglia in several models of neurodegenerative diseases, such as facial nerve axotomy⁸, scrapie^{10,11}, the methylphenyl-tetrahydro-pyridin model of Parkinson's disease¹⁴, Alzheimer's disease transgenic mice^{15,16} and toxic demyelination³². Recently, a critical role of bone marrow-derived microglia was attributed to their supposed function in restricting senile plaque formation in an amyloid β (A4) precursor protein/presenilin 1 mouse model of Alzheimer's disease⁵. This study further suggested that the bone marrow-derived cells selectively upregulated MHC class II and showed cell-specific phagocytic mechanisms of disease-associated

β -amyloid removal. It has further been reported that CCR2 deficiency renders mice more susceptible to Alzheimer's disease, most likely as a result of impaired amyloid degradation by brain endogenous phagocytes³⁹.

In contrast to an earlier report, in which bone marrow-derived monocytes and macrophages constituted up to 20% of the CD11b⁺ population during cuprizone-induced demyelination³², our data indicate that bone marrow-derived cells virtually do not contribute at all to the CD11b⁺/Iba-1⁺ population when the CNS was protected from irradiation. Thus, proliferation of endogenous microglia seems to be the most plausible explanation for the increase in Iba-1⁺ cell number. Indeed, local microglia proliferation in the lesioned CNS with intact blood-brain barrier has been reported^{11,40}.

It seems crucial to note that the vast majority of the bone-marrow chimera data were obtained from experiments using whole-body irradiation, without selective marrow-specific targeting of the myeloablating treatment. The involvement of the head during the irradiation procedure might have led to substantial local priming in the brain with concomitant induction of myeloattracting and myelopromoting factors and/or inactivation of inhibitory cues. Indeed, previous reports have already pointed to a local production of TNF α , IL-1 β and IL-6 in the irradiated rodent brain²⁸. We now demonstrate that, besides other cytokines and chemokines, the CCR2 ligand, CCL2, is produced as a result of the irradiation procedure. Because CCL2 is also induced during brain diseases⁴¹, this factor could be involved in the recruitment of CCR2-expressing myeloid cells into the CNS under several

conditions. Thus, it seems plausible that Ly-6C^{hi} monocytes equipped with CCR2 are preferentially recruited into the CNS, where they subsequently differentiate into microglia. The CCL2/CCR2 axis in general is thought to be the critical cue, as CCR2 was reported to be necessary for the egression of monocytes from the bone marrow to the spleen²⁵ and from the blood stream to the tissue²³. Nevertheless, it is possible that locally or distantly produced specific factors besides the investigated cytokines and chemokines are crucial for driving the recruitment of Ly-6C^{hi}CCR2⁺ monocytes into the CNS. In addition, subtle changes of blood-brain barrier integrity or inactivation of repulsory signals following irradiation might also promote cell engraftment.

Although we did not describe a role for Ly-6C^{lo}CCR2⁻ cells in the homeostasis of the brain or during disease, future studies may determine whether this monocyte subset, as possible precursors of dendritic cells²⁰, influences the adaptive arm of the immune system in the CNS, particularly with respect to antigen presentation and lymphocyte activation, processes that are known to occur in sterile CNS autoimmunity.

Taken together, our results identify Ly-6C^{hi}CCR2⁺ monocytes as direct precursors of microglia and point to the local factors in the CNS that are required for this process. Future studies will help to evaluate the impact of brain conditioning for directed myeloid cell targeting to the brain in therapeutic approaches for CNS diseases.

METHODS

Mice, generation of bone-marrow chimeric mice and adoptive transfer experiments. Bone-marrow chimeric mice were generated as described recently^{8,12,42–44}. We reconstituted 6–8-week-old C57BL/6 (*Ccr2*^{+/+}) recipient mice with BMCs derived from the tibias and femurs from adult ACTβ-EGFP mice alone (*Ccr2*^{+/+}GFP⁺)⁴⁵ or from double-mutant mice intercrossed with CCR2-deficient mice (*Ccr2*^{-/-}GFP⁺)²⁶. Specific body (protected) irradiation of mice was carried out by a 6-MV X-Ray Varian linear accelerator. Mice were put into a 20 × 20 × 3-cm cast perspex-lined chamber (5-mm gage, density of 1.18 g cm⁻³). Spiracles were provided and the heads of the mice were carefully adjusted to it. Mice were treated with parallel opposed fields with a maximum dose at a depth of 1.5 cm. The field size was adjusted to 14 × 20 cm, placing the brains of the mice outside of the irradiation fields, with only the body being irradiated with 1,100 cGy. A safety margin of 0.5 cm from the field border to the head was preserved, so that no dose could affect normal brain tissue. We injected 5 × 10⁶ *Ccr2*^{-/-}GFP⁺ or *Ccr2*^{+/+}GFP⁺ BMCs into the tail vein of recipients 24 h after irradiation. Reconstitution of total irradiated (unprotected) mice was carried out by mixing *Ccr2*^{-/-}GFP⁺ or *Ccr2*^{+/+}GFP⁺ BMCs in a 1:3 ratio with *Ccr2*^{+/+} BMCs, which resulted in similar reconstitution levels in all chimeric mice. CX₃CR1^{GFP/+} mice were a kind gift of D. Littman (New York University School of Medicine)⁴⁶. C57BL/10SgSnAi Rag2 common gamma chain mice were purchased from Taconic Europe. Reconstitution was assessed 6–8-weeks after grafting by FACS analysis of peripheral blood. Depletion of Ly-6C^{hi} monocytes was carried out with an antibody to CCR2 (MC-21)⁴⁷ or the corresponding isotype control 2 h after each cell injection. We injected 50 μg of antibodies intraperitoneally.

Quantification of microglia and macrophage engraftment in the CNS. After transcardial perfusion with phosphate-buffered saline and subsequent 4% paraformaldehyde, we obtained 20-μm cryosections from the brains. Primary and preabsorbed antibodies were added overnight at a dilution of 1:100 for Iba-1 (WACO), 1:50 for F4/80 (Serotec), 1:100 for NeuN (Chemicon International). Cy3-conjugated secondary antibodies (Dianova) were added at a dilution of 1:100 for Iba-1 and 1:600 for the other antibodies for 1 h. Nuclei were counterstained with 4,6-diamidino-2-phenylindole (DAPI). GFP-expressing ramified cells and Iba-1⁺ or F4/80⁺ macrophages and microglia were counted in at least three sections of each individual mouse. The number and the area occupied by engrafted cells were examined microscopically using a 200× microscopical magnification using a conventional fluorescence microscope (Olympus BX-51) equipped with a color camera (Olympus DP71).

Cuprizone treatment and facial nerve axotomy. Cuprizone experiments were carried out on 9–10-week-old chimeric mice. Mice were fed for 5 weeks with 0.2% (weight/weight) cuprizone (Sigma) in the ground breeder chow. Histopathological analysis using LFB staining for demyelination and GFAP immunohistochemistry for astrocytes was carried out as previously described⁴⁸. Unilateral facial nerve axotomy was induced in bone-marrow chimeras (created with unmixed GFP⁺ bone marrow) 4–6 weeks post-transplantation by transection of the facial nerve at the stylomastoid foramen, resulting in ipsilateral whisker paresis. Mice were killed for analysis after 14 d.

Microglia isolation. Murine microglia from adult mice were harvested using a percoll gradient as previously described⁴⁹. For culture experiments, primary microglia were prepared from newborn mice as described⁵⁰. For stimulation, microglial cells were seeded at a density of 2 × 10⁵ cells per well, and different concentrations of LPS or Pam₃CSK₄ were added to the cell culture medium for 18 h. Afterwards, TNFα and IL-6 enzyme-linked immunosorbent assays (ELISA) were carried out according to the manufacturer's instructions (R&D Systems). For MHC class II induction, cells were stimulated with IFNγ (20 ng ml⁻¹) alone or in combination with IFNβ (100 U ml⁻¹) for 18 h. For measurement of myelin phagocytosis, fluorescein isothiocyanate-labeled myelin was exposed to microglia at a protein concentration of 4 μg ml⁻¹ for 1 or 2 h alone or in the presence of cytochalasin D (5 μM). For microglia proliferation, culture medium was supplemented with different concentrations of recombinant mouse M-CSF (R&D Systems). After 48h, 10 μM BrdU (Sigma) was added for 1 h. Cells were fixed in 4% paraformaldehyde and stained with the BrdU *in situ* detection kit according to the manufacturer's instructions (BD Pharmingen).

Real-time PCR. RNA was extracted from the brains and spinal cords at indicated time points after or without irradiation. The tissue was flushed with ice-cold Hank's buffered salt solution, and RNA was isolated using RNeasy Mini kits (Qiagen) following the manufacturer's instructions. The samples were treated with DNaseI (Roche), and 1 μg of RNA was transcribed into cDNA using oligo-dT primers and the SuperScript II RT kit (Invitrogen). We transferred 2.5 μl cDNA into a 96-well Multiply PCR-plate (Sarstedt) and 12.5 μl Absolute QPCR SYBR Green master mix (ABgene) with 9.6 μl ddH₂O was added. The PCR reaction was carried out as previously described⁴³.

Statistical analysis. Statistical differences of clinical scores were evaluated using a nonpaired Student's *t* test. Differences were considered significant for *P* < 0.05.

Note: Supplementary information is available on the Nature Neuroscience website.

ACKNOWLEDGMENTS

We thank O. Kowatsch, M. Schedensack, E. Pralle, P. Grämmel and S. Blumenau for excellent technical assistance. We thank S. Jung (Rehovot, Israel) for scientific input. This work was supported by grants from Gemeinnützige Hertie-Stiftung to M.P. and D.M., Deutsche Forschungsgemeinschaft (SFB 507 A5 and PR 577) to J.P. and M.P. This project was supported by the DFG research Center for Molecular Physiology of the Brain Göttingen, but support was unfortunately discontinued. M.H. is supported by the Swiss MS Society and the Prof. Dr. Max-Cloëtta Foundation. A.M. and H.S. are fellows of the Gertrud Reemtsma Foundation.

AUTHOR CONTRIBUTIONS

A.M., H.S., M.N., D.M., U.-K.H., J.P. and M.P. conducted the experiments. M.M., M.H. and W.B. provided reagents and scientific input. A.M., J.P. and M.P. designed the experiments and wrote the manuscript.

Published online at <http://www.nature.com/natureneuroscience>
Reprints and permissions information is available online at <http://npj.nature.com/reprintsandpermissions>

- Hanisch, U.K. Microglia as a source and target of cytokines. *Glia* **40**, 140–155 (2002).
- Nimmerjahn, A., Kirchhoff, F. & Helmchen, F. Resting microglial cells are highly dynamic surveillants of brain parenchyma *in vivo*. *Science* **308**, 1314–1318 (2005).
- Davalos, D. *et al.* ATP mediates rapid microglial response to local brain injury *in vivo*. *Nat. Neurosci.* **8**, 752–758 (2005).

4. Streit, W.J., Walter, S.A. & Pennell, N.A. Reactive microgliosis. *Prog. Neurobiol.* **57**, 563–581 (1999).
5. Simard, A.R., Soulet, D., Gowing, G., Julien, J.P. & Rivest, S. Bone marrow-derived microglia play a critical role in restricting senile plaque formation in Alzheimer's disease. *Neuron* **49**, 489–502 (2006).
6. Hickey, W.F. & Kimura, H. Perivascular microglial cells of the CNS are bone marrow-derived and present antigen *in vivo*. *Science* **239**, 290–292 (1988).
7. Hickey, W.F., Vass, K. & Lassmann, H. Bone marrow-derived elements in the central nervous system: an immunohistochemical and ultrastructural survey of rat chimeras. *J. Neuropathol. Exp. Neurol.* **51**, 246–256 (1992).
8. Priller, J. *et al.* Targeting gene-modified hematopoietic cells to the central nervous system: use of green fluorescent protein uncovers microglial engraftment. *Nat. Med.* **7**, 1356–1361 (2001).
9. Wehner, T. *et al.* Bone marrow-derived cells expressing green fluorescent protein under the control of the glial fibrillary acidic protein promoter do not differentiate into astrocytes *in vitro* and *in vivo*. *J. Neurosci.* **23**, 5004–5011 (2003).
10. Williams, A.E., Lawson, L.J., Perry, V.H. & Fraser, H. Characterization of the microglial response in murine scrapie. *Neuropathol. Appl. Neurobiol.* **20**, 47–55 (1994).
11. Priller, J. *et al.* Early and rapid engraftment of bone marrow-derived microglia in scrapie. *J. Neurosci.* **26**, 11753–11762 (2006).
12. Djukic, M. *et al.* Circulating monocytes engraft in the brain, differentiate into microglia and contribute to the pathology following meningitis in mice. *Brain* **129**, 2394–2403 (2006).
13. Heppner, F.L. *et al.* Experimental autoimmune encephalomyelitis repressed by microglial paralysis. *Nat. Med.* **11**, 146–152 (2005).
14. Kokovay, E. & Cunningham, L.A. Bone marrow-derived microglia contribute to the neuroinflammatory response and express iNOS in the MPTP mouse model of Parkinson's disease. *Neurobiol. Dis.* **19**, 471–478 (2005).
15. Malm, T.M. *et al.* Bone marrow-derived cells contribute to the recruitment of microglial cells in response to beta-amyloid deposition in APP/PS1 double transgenic Alzheimer mice. *Neurobiol. Dis.* **18**, 134–142 (2005).
16. Stalder, A.K. *et al.* Invasion of hematopoietic cells into the brain of amyloid precursor protein transgenic mice. *J. Neurosci.* **25**, 11125–11132 (2005).
17. Massengale, M., Wagers, A.J., Vogel, H. & Weissman, I.L. Hematopoietic cells maintain hematopoietic fates upon entering the brain. *J. Exp. Med.* **201**, 1579–1589 (2005).
18. van Furth, R. & Cohn, Z.A. The origin and kinetics of mononuclear phagocytes. *J. Exp. Med.* **128**, 415–435 (1968).
19. Gordon, S. & Taylor, P.R. Monocyte and macrophage heterogeneity. *Nat. Rev. Immunol.* **5**, 953–964 (2005).
20. Geissmann, F., Jung, S. & Littman, D.R. Blood monocytes consist of two principal subsets with distinct migratory properties. *Immunity* **19**, 71–82 (2003).
21. Grage-Griebenow, E., Flad, H.D. & Ernst, M. Heterogeneity of human peripheral blood monocyte subsets. *J. Leukoc. Biol.* **69**, 11–20 (2001).
22. Sunderkotter, C. *et al.* Subpopulations of mouse blood monocytes differ in maturation stage and inflammatory response. *J. Immunol.* **172**, 4410–4417 (2004).
23. Swirski, F.K. *et al.* Ly-6Chi monocytes dominate hypercholesterolemia-associated monocyteosis and give rise to macrophages in atheromata. *J. Clin. Invest.* **117**, 195–205 (2007).
24. Sedgwick, J.D. *et al.* Isolation and direct characterization of resident microglial cells from the normal and inflamed central nervous system. *Proc. Natl. Acad. Sci. U.S.A.* **88**, 7438–7442 (1991).
25. Serbina, N.V. & Pamer, E.G. Monocyte emigration from bone marrow during bacterial infection requires signals mediated by chemokine receptor CCR2. *Nat. Immunol.* **7**, 311–317 (2006).
26. Kuziel, W.A. *et al.* Severe reduction in leukocyte adhesion and monocyte extravasation in mice deficient in CC chemokine receptor 2. *Proc. Natl. Acad. Sci. U.S.A.* **94**, 12053–12058 (1997).
27. Furuya, T. *et al.* Establishment of modified chimeric mice using GFP bone marrow as a model for neurological disorders. *Neuroreport* **14**, 629–631 (2003).
28. Linard, C. *et al.* Acute induction of inflammatory cytokine expression after gamma-irradiation in the rat: effect of an NF-kappaB inhibitor. *Int. J. Radiat. Oncol. Biol. Phys.* **58**, 427–434 (2004).
29. Francois, S. *et al.* Local irradiation not only induces homing of human mesenchymal stem cells at exposed sites but promotes their widespread engraftment to multiple organs: a study of their quantitative distribution after irradiation damage. *Stem Cells* **24**, 1020–1029 (2006).
30. Kondo, A., Nakano, T. & Suzuki, K. Blood-brain barrier permeability to horseradish peroxidase in twitcher and cuprizone-intoxicated mice. *Brain Res.* **425**, 186–190 (1987).
31. Bakker, D.A. & Ludwin, S.K. Blood-brain barrier permeability during Cuprizone-induced demyelination. Implications for the pathogenesis of immune-mediated demyelinating diseases. *J. Neurol. Sci.* **78**, 125–137 (1987).
32. McMahon, E.J., Suzuki, K. & Matsushima, G.K. Peripheral macrophage recruitment in cuprizone-induced CNS demyelination despite an intact blood-brain barrier. *J. Neuroimmunol.* **130**, 32–45 (2002).
33. Alliot, F., Godin, I. & Pessac, B. Microglia derive from progenitors, originating from the yolk sac, and which proliferate in the brain. *Brain Res. Dev. Brain Res.* **117**, 145–152 (1999).
34. Wegiel, J. *et al.* Reduced number and altered morphology of microglial cells in colony stimulating factor-1-deficient osteopetrotic op/op mice. *Brain Res.* **804**, 135–139 (1998).
35. Beers, D.R. *et al.* Wild-type microglia extend survival in PU.1 knockout mice with familial amyotrophic lateral sclerosis. *Proc. Natl. Acad. Sci. USA* **103**, 16021–16026 (2006).
36. Vallieres, L. & Sawchenko, P.E. Bone marrow-derived cells that populate the adult mouse brain preserve their hematopoietic identity. *J. Neurosci.* **23**, 5197–5207 (2003).
37. Simard, A.R. & Rivest, S. Bone marrow stem cells have the ability to populate the entire central nervous system into fully differentiated parenchymal microglia. *FASEB J.* **18**, 998–1000 (2004).
38. Biffi, A. *et al.* Correction of metachromatic leukodystrophy in the mouse model by transplantation of genetically modified hematopoietic stem cells. *J. Clin. Invest.* **113**, 1118–1129 (2004).
39. El Khoury, J. *et al.* Ccr2 deficiency impairs microglial accumulation and accelerates progression of Alzheimer-like disease. *Nat. Med.* **13**, 432–438 (2007).
40. Remington, L.T., Babcock, A.A., Zehntner, S.P. & Owens, T. Microglial recruitment, activation and proliferation in response to primary demyelination. *Am. J. Pathol.* **170**, 1713–1724 (2007).
41. Yamamoto, M. *et al.* Overexpression of monocyte chemoattractant protein-1/CCL2 in beta-amyloid precursor protein transgenic mice show accelerated diffuse beta-amyloid deposition. *Am. J. Pathol.* **166**, 1475–1485 (2005).
42. Prinz, M. *et al.* Positioning of follicular dendritic cells within the spleen controls prion neuroinvasion. *Nature* **425**, 957–962 (2003).
43. Prinz, M. *et al.* Innate immunity mediated by TLR9 modulates pathogenicity in an animal model of multiple sclerosis. *J. Clin. Invest.* **116**, 456–464 (2006).
44. Greter, M. *et al.* Dendritic cells permit immune invasion of the CNS in an animal model of multiple sclerosis. *Nat. Med.* **11**, 328–334 (2005).
45. Okabe, M., Ikawa, M., Kominami, K., Nakanishi, T. & Nishimune, Y. 'Green mice' as a source of ubiquitous green cells. *FEBS Lett.* **407**, 313–319 (1997).
46. Jung, S. *et al.* Analysis of fractalkine receptor CX3CR1 function by targeted deletion and green fluorescent protein reporter gene insertion. *Mol. Cell. Biol.* **20**, 4106–4114 (2000).
47. Mack, M. *et al.* Expression and characterization of the chemokine receptors CCR2 and CCR5 in mice. *J. Immunol.* **166**, 4697–4704 (2001).
48. Merkler, D. *et al.* Multicontrast MRI of remyelination in the central nervous system. *NMR Biomed.* **18**, 395–403 (2005).
49. van Loo, G. *et al.* Inhibition of transcription factor NF-kappaB in the central nervous system ameliorates autoimmune encephalomyelitis in mice. *Nat. Immunol.* **7**, 954–961 (2006).
50. Prinz, M. & Hanisch, U.K. Murine microglial cells produce and respond to interleukin-18. *J. Neurochem.* **72**, 2215–2218 (1999).